NASA TECHNICAL MEMORANDUM

NASA TM X-73,097

NASA TM X-73,097

AIRFOIL SECTION DRAG REDUCTION AT TRANSONIC SPEEDS BY NUMERICAL OPTIMIZATION

Raymond M. Hicks, Garret N. Vanderplaats

Ames Research Center
Moffett Field, Calif. 94035

Earll M. Murman

Flow Research, Inc.
Kent, Washington

and

Rosa R. King

Computer Sciences Corp.
Mountain View, California

February 1976

1. Report No.	2. Government Accession No.	3. Recipient's Catalog No.
TM X-73,097		

4. Title and Subtitle	5. Report Date
AIRFOIL SECTION DRAG REDUCTION AT TRANSONIC SPEEDS BY NUMERICAL OPTIMIZATION	6. Performing Organization Code

7. Author(s)	8. Performing Organization Report No.
Raymond M. Hicks, Garret N. Vanderplaats, Earll M. Murman,* and Rosa R. King†	A-6407

9. Performing Organization Name and Address	10. Work Unit No.
Ames Research Center, Moffett Field, Calif. 94035 *Flow Research, Inc., Kent, Washington †Computer Sciences Corp., Mountain View, Calif.	505-06-31
	11. Contract or Grant No.
	13. Type of Report and Period Covered: Technical Memorandum
12. Sponsoring Agency Name and Address National Aeronautics and Space Administration Washington, D. C. 20546	14. Sponsoring Agency Code

15. Supplementary Notes

16. Abstract

A practical procedure for the design of low drag, transonic airfoils is demonstrated. The procedure uses an optimization program, based on a gradient algorithm coupled with an aerodynamic analysis program, that solves the full, non-linear potential equation for transonic flow. The procedure is useful for the design of retrofit modifications for drag reduction of existing aircraft as well as for the design of low drag profiles for new aircraft. Results are presented for the modification of four different airfoils to decrease the drag at a given transonic Mach number.

17. Key Words (Suggested by Author(s))	18. Distribution Statement
Aerodynamics Airfoil Wing Airplane design Computer design	Unlimited STAR Category - 02

19. Security Classif. (of this report)	20. Security Classif. (of this page)	21. No. of Pages	22. Price*
Unclassified	Unclassified	32	$3.75

*For sale by the National Technical Information Service, Springfield, Virginia 22151

NOMENCLATURE

a_i = design variables for the upper surface, $i = 1,7$

b_i = design variables for the lower surface, $i = 1,7$

C_d = section drag coefficient

C_l = section lift coefficient

C_m = section pitching-moment coefficient, referenced to quarter-chord point

C_p = pressure coefficient, $(p_1-p)/q$

C_p^* = pressure coefficient corresponding to a local Mach number of 1

c = chord

M = Mach number

p = free-stream static pressure

p_1 = local static pressure

q = free stream dynamic pressure

Re = Reynolds number

$\bar{s}$ = move direction vector

x = chordwise distance

y = vertical distance

α = angle of attack

Subscripts

inv = inviscid

ls = lower surface

max = maximum

min = minimum

us = upper surface

visc = viscous

THE WORLDWIDE FUEL SHORTAGE has prompted new interest in reducing the fuel consumption of existing and future aircraft and a logical place to begin is by reducing drag. At transonic speeds drag reduction can be accomplished by eliminating or weakening rapid recompressions or shock waves over the aircraft surfaces. In particular, the wing profile can often be redesigned to achieve drag reduction.

Several methods are available to aid the designer in developing advanced airfoil sections (e.g., the hodograph method (1,2),* an inverse method applied in the physical plane (3), and a combined inverse-direct method (4). However, the hodograph procedure is complicated and its application requires extensive experience in applied mathematics and theoretical fluid mechanics. The inverse method requires an a priori knowledge of the desirable form of the pressure or velocity distribution, and constraints are not readily imposed. The combination inverse-direct method is complicated and requires a designer in the "loop" to monitor and enhance the convergence of the optimization process to a realistic airfoil shape.

In this report the numerical optimization design technique (5-8) has been extended to the design of lifting transonic airfoils. The numerical optimization design technique uses two existing computer programs: an optimization program based on the method of feasible directions (9) and an aerodynamics analysis program based on an iterative solution of the full potential equation for transonic flow (10). The optimization procedure can be used to design airfoil sections for any speed regime from low speed through transonic with geometric or aerodynamic constraints. Several examples of the application of the procedure to the design of low-drag transonic airfoils are given. It should be noted that the results presented here are preliminary and are intended only to illustrate the usefulness and simplicity of the technique.

DESIGN METHOD

The program organization of the numerical optimization design technique used in this

*Numbers in parentheses designate References at end of paper.

study is shown in Fig. 1. The initial airfoil required to start each design problem is obtained by fitting a polynomial to that region of the airfoil to be modified, or to the entire airfoil if a complete new profile is desired. The coefficients of such a polynomial are the design variables perturbed by the optimization program to achieve the desired design improvement. If a 6th degree polynomial representation of the airfoil geometry is used, the coefficients for the starting airfoil are obtained by fitting the polynomials to seven points on the upper surface and to seven points on the lower surface of a known suitable airfoil section. The coefficients, along with the Mach number, angle of attack, and constraints are the required inputs to start the optimization process.

If the problem being considered is pitching-moment minimization, the optimization program perturbs the polynomial coefficients one by one, returning to the aerodynamics program for evaluation of the pitching moment after each perturbation. After all coefficients have been perturbed and the direction of change of the pitching moment has been noted for each polynomial coefficient change, the optimization program then calculates the partial derivatives (by one-sided finite difference) of moment with respect to each polynomial coefficient, thus forming the gradient of the pitching moment (∇C_m). The direction in which the polynomial coefficients are changed to reduce the nose-down pitching moment is $-\nabla C_m$ (the steepest descent direction). The optimization program then increments the polynomial coefficients one to four times in the direction indicated by $-\nabla C_m$. The program searches in this direction until the moment starts to increase (because of nonlinearity in the design space) or a constraint is encountered. If either of these possibilities occurs, new gradients are calculated and a new direction is found that will decrease pitching moment without violating any constraints. When a minimum value of pitching moment is reached with no violated constraints, the coordinates of the final airfoil are printed, together with the final pressure distribution and aerodynamic coefficients.

A graphic presentation of a hypothetical optimization problem using two design variables is shown in Fig. 2. Assume that the optimization problem to be attempted is minimization of drag coefficient with constraints on lift coefficient and airfoil thickness, and with the airfoil geometry described by the polynomials shown in the figure. In this case,

the optimization program is allowed to perturb only a_1 and a_2 to achieve the desired drag reduction. This permits only a limited reshaping of the upper surface. Note that the thickness constraint is a straight line (that is, a linear function of the polynomial coefficients) whereas the lift constraint is nonlinear. The optimization program can handle both linear and nonlinear constraints efficiently.

The design space is divided into two regions, an infeasible region where one or both constraints are violated, and a feasible region where no constraints are violated. Minimum drag in the feasible region is sought. Assumed starting values of a_1 and a_2 are depicted by point A. The gradient of drag (∇C_d) is calculated for this point, giving the direction of change in a_1 and a_2 as $\bar{s} = -\nabla C_d$. In this case, both a_1 and a_2 must be decreased to minimize drag. Movement in direction $\bar{s}$ continues until the lift constraint is encountered at point B. At this point, the gradient of lift (∇C_ℓ) is required along with ∇C_d to define a new direction $\bar{s}$. Now a_1 must be increased and a_2 must be decreased to minimize drag by moving along the lift constraint. The optimum is shown as the point where the line of constant drag with least value in the feasible region intersects the lift constraint.

If the starting values of a_1 and a_2 are given by point C (Fig. 2), the problem begins in the infeasible region. Now a direction $\bar{s}$ is determined that moves toward the feasible region with a minimum increase in drag, while overcoming the violated lift constraint. Such a move requires an increase in both a_1 and a_2. When the feasible region is reached, a direction $\bar{s}$ is then determined that will move along the lift constraint until the optimum is attained. A more complete discussion of airfoil design by numerical optimization is given in reference 8.

DESIGN RESULTS AND DISCUSSION

All design problems considered during this study consisted of modifying the upper surface of an existing airfoil section to achieve transonic drag reduction. The equation used to describe that portion of the upper surface to be modified is the following cubic equation:

$$y = a_1(x/c)^{a_4} + k(x/c) + a_2(x/c)^2 + a_3(x/c)^3 \quad (1)$$

The coefficient, k, is used to match ordinates at the chordwise station where the forward region of the airfoil to be modified ends and the fixed aft region begins. When the entire upper surface is to be modified, the coefficient, k, is used to fix the trailing edge bluntness. The design variables are the coefficients, a_1-a_3, and the exponent, a_4. The starting value of a_4 was 0.5 for all initial airfoil sections considered. The final value of a_4 depends on the amount of leading edge bluntness required to achieve drag reduction. Each airfoil modification reported here was found to need more leading edge bluntness than exhibited by the starting airfoil to achieve the desired drag reduction and hence the final value of a_4 was less than 0.5 in each case.

While substantial drag reductions were achieved by using equation (1), the development of shock-free sections was difficult because of the restricted class of sections that can be described by such an equation. Additional work is needed to obtain more general geometric representations for transonic airfoil design. In particular, equations are needed that will allow decoupling of various regions of the airfoil surface without permitting waviness to develop. The inability to develop shock-free sections may not be a serious limitation of the method, however, since the off-design characteristics of such sections are often poor in comparison to weak-shock sections. In each case presented here the shock strength was sufficiently weakened to prevent shock-induced boundary layer separation from occurring at the design condition (i.e., the shock-Mach number was reduced to at least 1.2 in each case).

In reference to the figures cited below, only upper surface pressure distributions are shown when the presentation is clarified by omitting lower surface pressures. (There were only slight changes in the lower surface pressures when the upper surface was modified.)

CASE I. UPPER SURFACE MODIFICATION OF AN APPROXIMATE NACA 6-SERIES PROFILE - The results of modifying the upper surface of an airfoil to achieve drag reduction at $M = 0.7$ are shown in Fig. 3. The initial airfoil is an approximation to a 13-percent thick NACA 6-series section. The lower surface is exact and the upper surface is represented by equation (1). The drag coefficient given in the figure is

obtained by a surface pressure integral and represents the drag due to shock losses in an inviscid flow. Note that the drag coefficient is reduced to approximately one-fourth that of the initial airfoil. The drag reduction is accompanied by a reduction in nose-down pitching moment, a small loss in lift, and a redistribution of the area contained within the profile contour. A constraint on the cross-sectional area ("volume") of the profile prevented further thinning of the section to achieve the drag reduction. Note the substantial reduction in shock strength and the forward movement of the shock position.

The aerodynamic characteristics of the two airfoils of Fig. 3, corrected for viscosity, are shown at Reynolds numbers of 1.3×10^6 and 20×10^6 in Figs. 4(a) and 4(b), respectively. The boundary layer characteristics were calculated by a theory described in reference 10. This theory uses an inviscid pressure distribution as input to the von Karman momentum equation which, when integrated, gives the boundary layer displacement thickness. This displacement thickness is smoothed and added to the airfoil contour to account for a turbulent boundary layer. The displacement thickness correction is computed iteratively with the flow calculation. As expected, the lift and pitching moment coefficients show the typical decambering effect of the boundary layer; namely, the coefficients for viscous flow are smaller than the corresponding coefficients for inviscid flow. Note that the drag reduction due to modification of the airfoil contour is smaller when the boundary layer correction is included in the calculation; nevertheless, a substantial reduction still is achieved. The aerodynamic coefficients shown in Fig. 4(b) at a Reynolds number of 20×10^6 are somewhat closer to the corresponding inviscid values because of the smaller boundary layer thickness at the higher Reynolds number. Again, a substantial drag reduction is noted.

A graph of C_d vs Mach number at $\alpha = 0°$ for the initial and final profiles of Fig. 3 is shown in Fig. 5 for a Reynolds number of 20×10^6. The drag divergence Mach number is increased by approximately 0.04 by the contour reshaping shown in Fig. 3. It is interesting to note that this type of re-contouring to reduce shock drag at transonic speeds does not produce a drag penalty for subsonic flow or a more rapid drag rise above the design Mach number ($M = 0.7$).

Plots of low speed (M = 0.1) pressure distributions for $\alpha = 10^{\circ}$ are given in Fig. 6 for both of the airfoils shown in Fig. 3. The low speed aerodynamic characteristics were evaluated for the airfoil shown in Fig. 6 and for the next two profile modifications (Figs. 7 and 11) to investigate the compatibility of section re-contouring for transonic drag reduction with low speed, high lift requirements. Note that the pressure peak near the leading edge on the upper surface is reduced by more than a factor of 2 by increasing the leading edge bluntness of the 'initial' airfoil shown in Fig. 3. Moreover, the adverse pressure gradient following the leading edge pressure peak is substantially reduced, thereby improving maximum lift and low-speed handling.

CASE II. FORWARD UPPER SURFACE MODIFICATION OF AN APPROXIMATE NACA 6-SERIES PROFILE - The results of modifying the forward 35 percent of the upper surface of a 12-percent thick NACA 6-series section to reduce shock drag at M = 0.72 are shown in Fig. 7. Again, a substantial reduction in drag is achieved along with a smaller nose-down pitching moment and little change in lift coefficient. The slight irregularity in the pressure distribution near the 38-percent chord station is due to a slight mismatch in the first derivative of the contour at the point where the forward section described by equation (1) joined the fixed aft section of the airfoil. Such irregularities can arise because the only boundary conditions imposed on the geometry of the upper surface were matched ordinates at the end of the forward section.

The aerodynamic characteristics of the airfoil sections of Fig. 7, corrected for viscosity, are shown in Figs. 8(a) and 8(b) for Reynolds numbers of 1.3×10^6 and 20×10^6, respectively. As noted for the preceding case (Figs. 3 and 4), the lift and pitching moment coefficients are reduced due to the decambering effect of the boundary layer. The reduction in drag is smaller when viscous effects are included but still large enough to warrant consideration of such contour modification for retrofit of existing aircraft.

The effect of Mach number on the drag characteristics of the airfoils of Fig. 7 is shown in Fig. 9 for a Reynolds number of 20×10^6. As for the preceding case (Figs. 3-6), no drag penalty is incurred at subcritical

Mach numbers by the type of contour modifications considered here. The drag divergence Mach number is increased by approximately 0.02 with similar drag rise characteristics above the design point ($M = 0.72$) for both airfoil sections.

The low speed pressure distributions at high angles of attack for the two sections of Fig. 7 are shown in Fig. 10. As noted in the previous case (Figs. 3-6), the increased leading edge bluntness of the modified section produced a reduced pressure peak, a smaller adverse pressure gradient and a rearward shift of the pressure peak. All these factors should increase the maximum lift coefficient and improve the low speed handling of aircraft incorporating this airfoil modification.

CASE III. FORWARD UPPER SURFACE MODIFICATION OF THE NACA 23015 PROFILE - The results of a forward upper surface contour modification designed to reduce the shock drag of the NACA 23015 airfoil section at $M = 0.7$ and $\alpha = 0°$ are shown in Fig. 11. In this case the initial airfoil shown in the figure and the corresponding upper surface pressure distribution represent the exact NACA 23015 profile rather than an approximation obtained by using equation (1), as was done for the initial airfoil in the two preceding NACA 6-series airfoil modifications. In this case the modified section is almost shock-free ($C_d = 0.0005$) and exhibits nearly the same pitching moment and lift coefficients as the original NACA 23015 section. The desired drag reduction was achieved with a smaller contour change than that made in the two preceding cases because the initial shock was weaker (compare Figs. 3 and 7 with Fig. 11).

The aerodynamic characteristics of the original and of the modified 23015 sections, corrected for viscosity, are shown in Fig. 12 for a Reynolds number of 10×10^6. Again, the same trend as noted for the two previous NACA 6-series modifications is noted: namely, the lift and pitching moment coefficients are reduced, relative to the inviscid values, due to viscous effects, and the percent reduction in drag is smaller.

The effect of Mach number on the drag characteristics of the modified and original NACA 23015 sections is shown in Fig. 13 for a Reynolds number of 20×10^6. The improved drag rise Mach number and drag rise characteristics exhibited by the modified 23015 section are similar to those noted earlier for the

modified 6-series sections (Figs. 5 and 9). However, the subsonic drag of the modified 23015 section is predicted to be somewhat less than that of the original NACA 23015 profile.

The low speed, high lift characteristics of the modified 23015 profile require a more careful analysis than the modified 6-series sections shown previously because the original NACA 23015 airfoil section exhibits one of the highest maximum lift coefficients of all NACA profiles that have similar design lift coefficients (11). The type of profile modification used in this study can generally be relied upon to improve the high lift characteristics of 6-series airfoils at low speed because most 6-series profiles have relatively small leading edge radii. However, when such modifications are applied to NACA 4- and 5- digit sections to reduce drag at transonic speeds, the low speed, maximum lift characteristics of the modified profiles may incur a slight penalty. Such a penalty can often be minimized or avoided, if the high lift characteristics are considered during the optimization process, by careful application of constraints on the design.

The inviscid, low speed pressure distributions for the NACA 23015 section and modified section are shown in Figs. 14 and 15, respectively, at four angles of attack from 0° to 15°. Analysis of these pressure distributions shows two interesting facts: first, the modified profile exhibits greater suction pressures than the original NACA 23015 section at all angles of attack shown, except at 0°; and second, the rate of growth of $C_{p_{min}}$ with angle of attack is smaller for the modified section than for the original section. This latter fact is illustrated more clearly in Fig. 16, which shows a graph of the ratio of minimum pressure coefficient for the modified section to minimum pressure coefficient for the original section vs angle of attack. Note, that the ratio decreases above $\alpha = 7°$. Since the stalling angle for the NACA 23015 section is between 15° and 18°, depending on Reynolds number (11), it is possible that the pressure coefficient ratio may reach a value of 1.0 before stall, and hence the maximum lift coefficient for the two profiles may be similar. A wind tunnel test would be the only means of providing positive evaluation of the high lift characteristics of the two profiles.

CASE IV. FORWARD UPPER SURFACE MODIFICATION OF THE NACA 64A109 PROFILE - The final drag minimization problem considered in this study was modification of the forward upper surface of the NACA 64A109 section for M = 0.82 (Fig. 17). The results of this modification are similar to those shown for the 6-series sections shown in Figs. 3 and 7; that is, the drag is substantially reduced along with a reduction in nose-down pitching moment and little change in lift coefficient. The off-design characteristics and low speed, high lift characteristics were not evaluated because of time limitations and the fact that the trends would be expected to be similar to those shown for the previous 6-series modifications. The initial profile and corresponding pressure distribution shown in the figure are those of the exact NACA 64A109 profile.

CONCLUDING REMARKS

A technique for achieving drag reduction of airfoil sections at transonic speed was demonstrated. When the method is applied to drag reduction of NACA 6-series sections, or to other profiles with small leading edge radii, the reduced drag is generally accompanied by a reduction in nose-down pitching moment, little change in lift coefficient for the design condition, and improved low speed, high lift characteristics.

When NACA 5-digit sections, or other profiles with larger leading edge radii, are modified to achieve drag reduction at transonic speeds, it was again found that the nose-down pitching moment was reduced; the lift coefficient remained about the same at the design condition. However, a more careful analysis of the low speed, high lift characteristics is required and some additional re-contouring of the profile may be required to insure adequate low speed aerodynamics.

Further work is needed to achieve more flexibility in the geometric representation used with the numerical optimization technique so that a wider range of modifications can be achieved.

Experimental verification of the type of modifications developed during this study is required before such designs can be considered for retrofit of existing aircraft or used in new aircraft.

The off-design characteristics of the four airfoil modifications developed during this study were good. Furthermore, it is expected that such off-design behavior is typical of the type of low drag, transonic airfoil section generated by the design technique presented in this report.

In all cases the modifications were developed by use of an inviscid aerodynamic theory to reduce computational cost. The aerodynamic characteristics of the initial and final profiles were verified by use of a theory that includes viscosity corrections.

A typical airfoil modification, including re-contouring by numerical optimization, verification of design by use of a theory corrected for viscosity, and evaluation of low speed, high lift characteristics required approximately 20 min of CPU time on a CDC 7600 computer.

REFERENCES

1. F. Bauer, P. Garabedian, and D. Korn, Lecture Notes in Economics and Mathematical Systems. "Supercritical Wing Sections," Vol. 66, Springer-Verlag, 1972.

2. G. Y. Nieuwland, "Transonic Potential Flow Around a Family of Quasi-Elliptical Aerofoil Sections." National Aerospace Laboratory, Technical Report T. 172, 1967.

3. B. Arlinger, "An Exact Method of Two Dimensional Airfoil Design." Saab TN 67, 1970.

4. Joseph L. Steger and John M. Klineberg, "A Finite Difference Method for Transonic Airfoil Design." AIAA Journal, Vol. 11, No. 5, May 1973.

5. Raymond M. Hicks, Earll M. Murman, and Garret N. Vanderplaats, "An Assessment of Airfoil Design by Numerical Optimization." NASA TM X-3092, 1974.

6. Raymond M. Hicks and Garret N. Vanderplaats, "Application of Numerical Optimization to the Design of Low-Speed Airfoils." NASA TM X-3213, 1975.

7. Raymond M. Hicks and Garret N. Vanderplaats, "Design of Low-Speed Airfoils by Numerical Optimization." SAE Paper 750574, 1975.

8. Garret N. Vanderplaats, Raymond M. Hicks, and Earll M. Murman, "Application of Numerical Optimization Techniques to Airfoil Design." NASA SP-347, 1975.

9. Garret N. Vanderplaats, "CONMIN-A Fortran Program for Constrained Function Minimization." NASA TM X-62,282, Aug. 1973.

10. F. Bauer, P. Garabedian, D. Korn, and A. Jameson, Lecture Notes in Economics and Mathematical Systems. "Supercritical Wing Sections II," Vol. 108, Springer-Verlag, 1975.

11. I. H. Abbott, A. E. von Doenhoff, and L. S. Stivers Jr., "Summary of Airfoil Data." NACA Report No. 824, 1945.

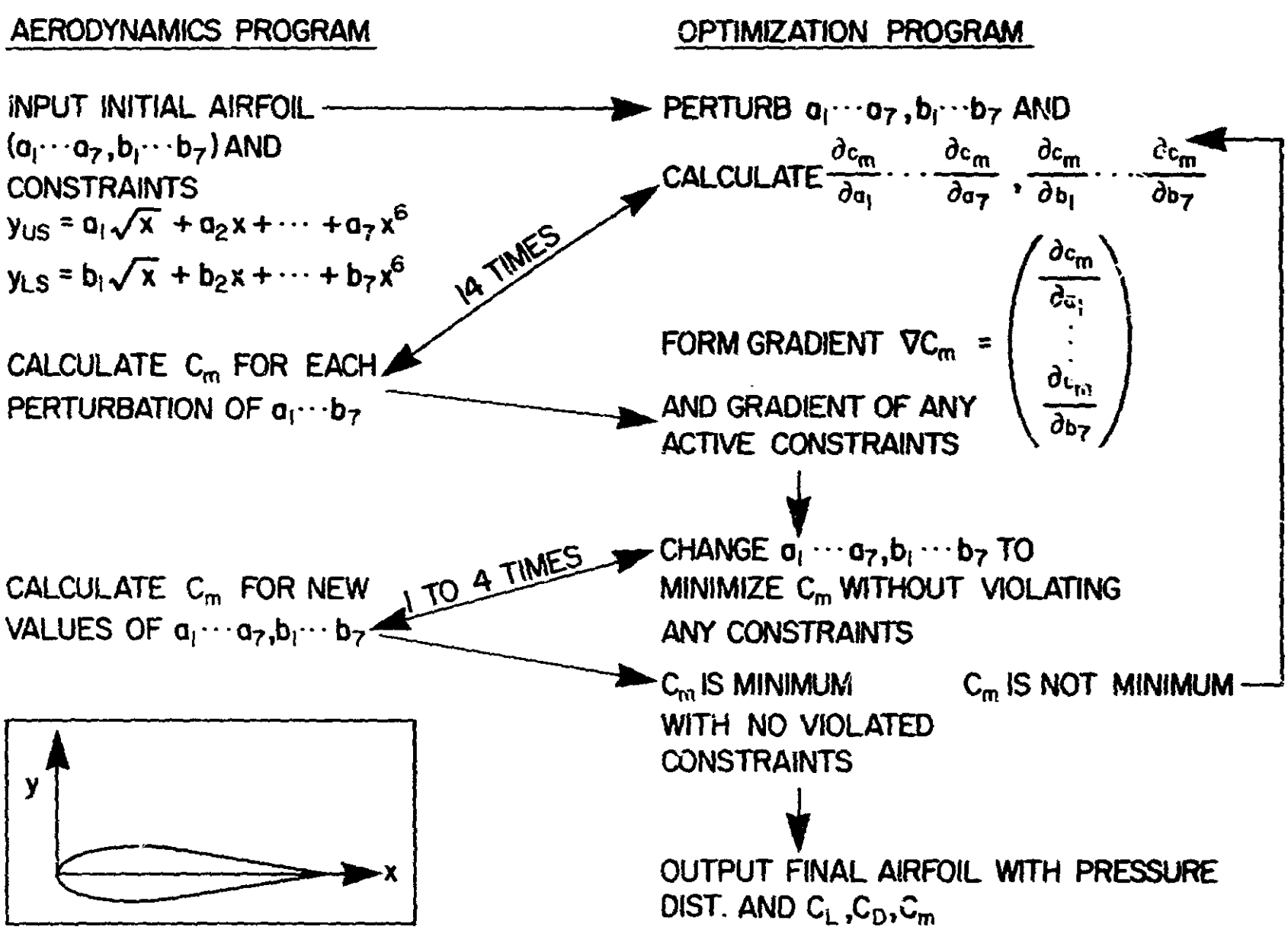

Fig. 1 - Program organization

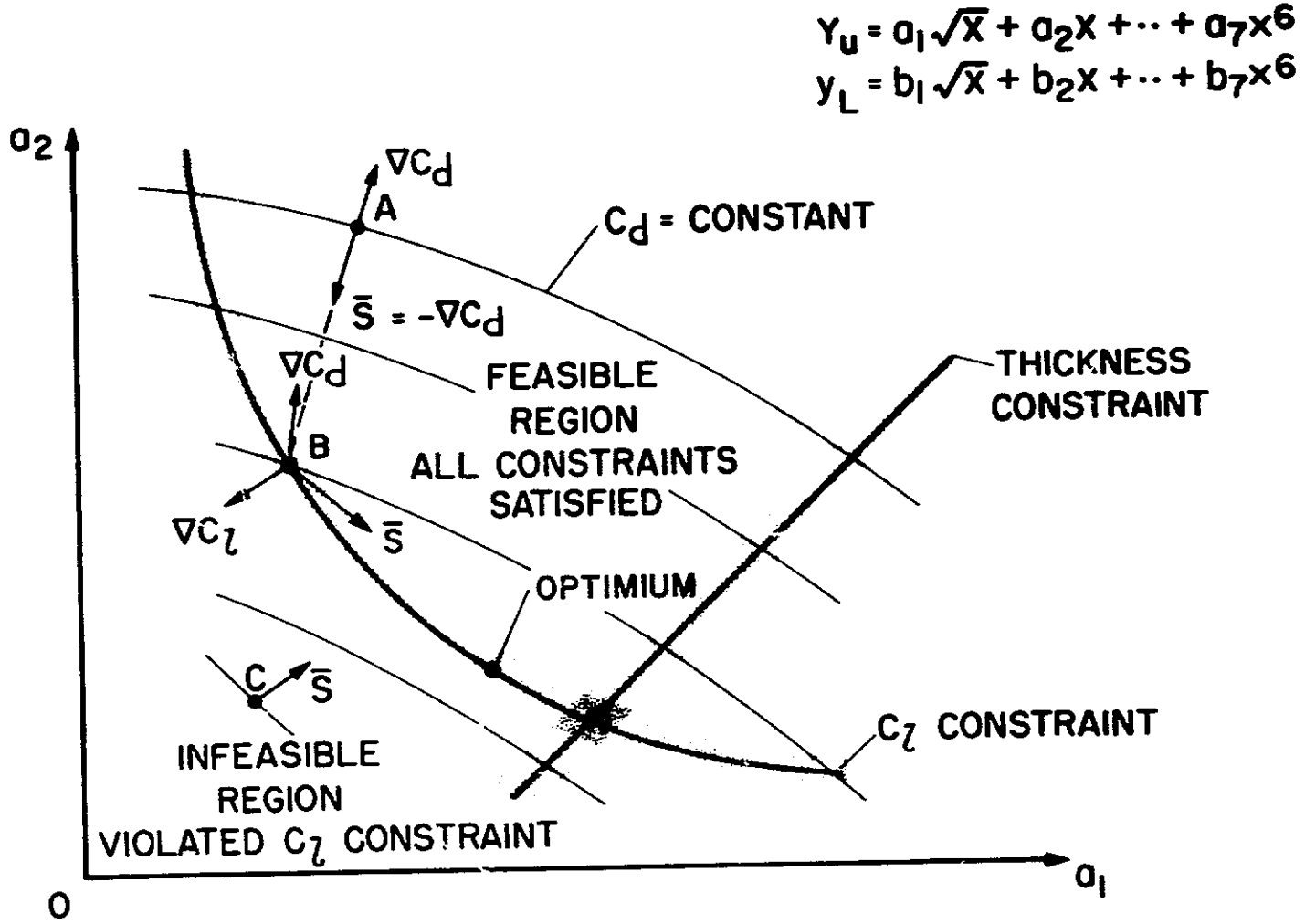

Fig. 2 - Two-variable design problem

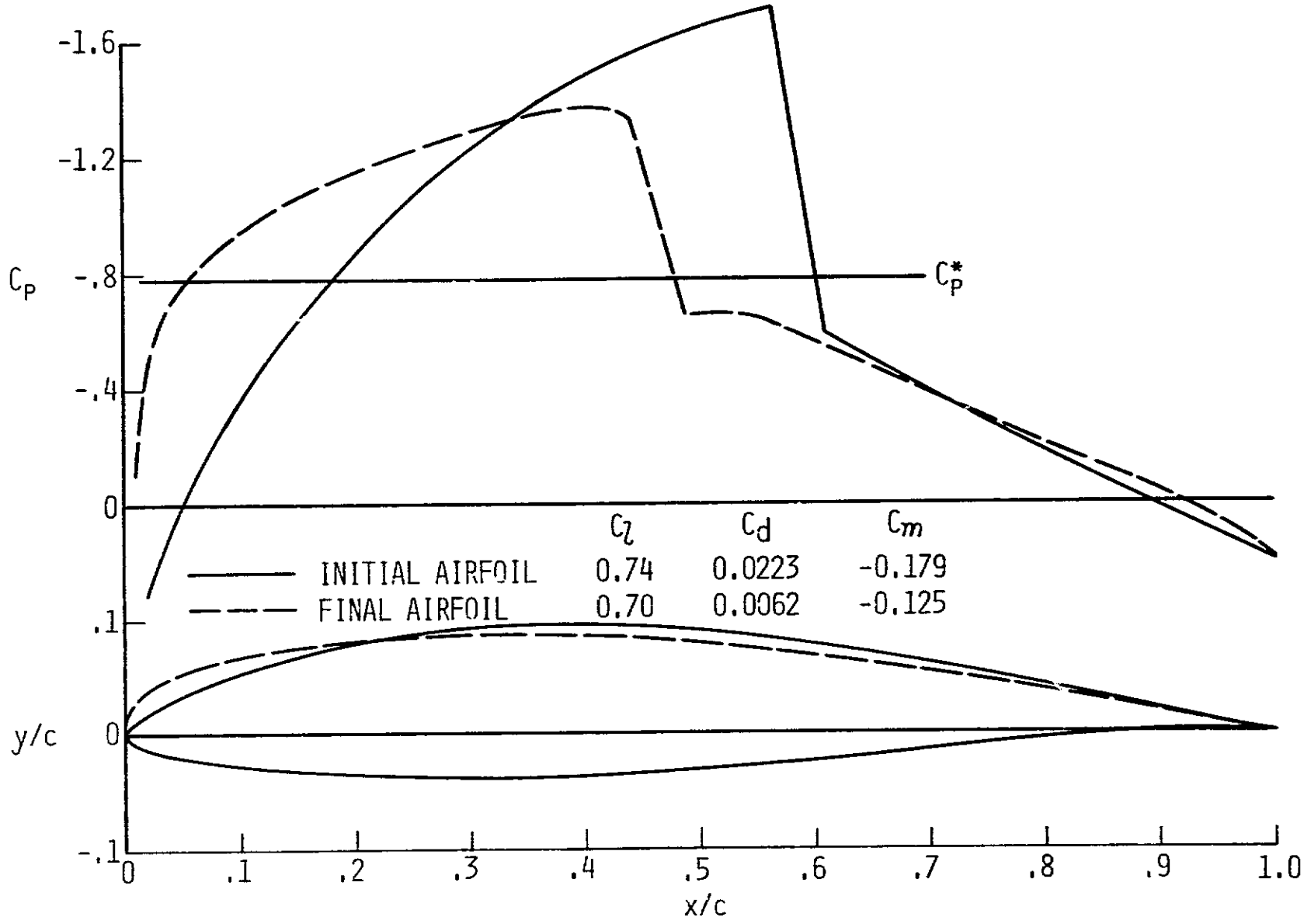

Fig. 3 - Inviscid drag minimization; M = 0.70, $\alpha = 0°$

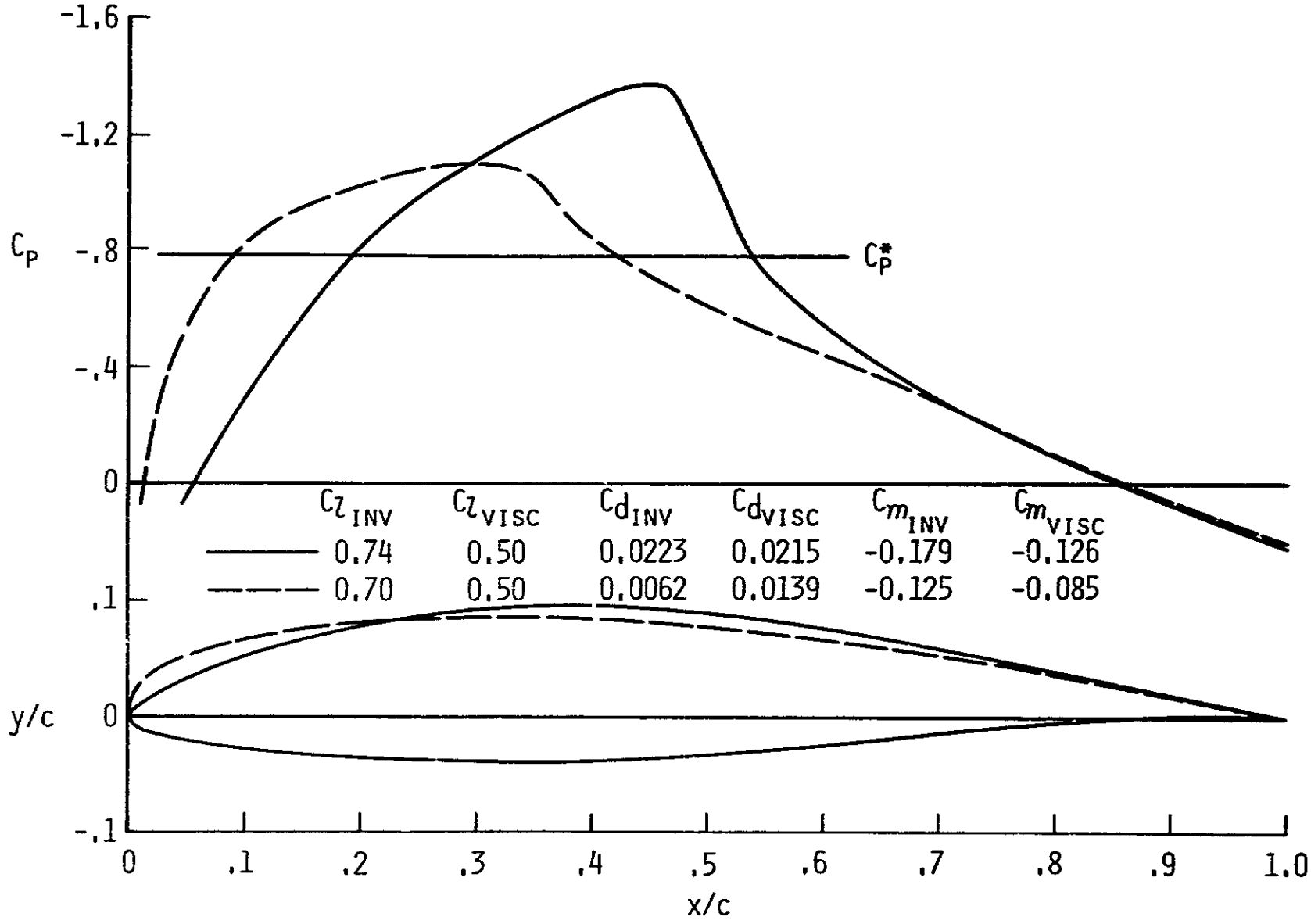

(a) Re = 1.3×10^6

Fig. 4 - Aerodynamic characteristics of the airfoils shown in figure 3 with boundary-layer correction; M = 0.7, $\alpha = 0°$

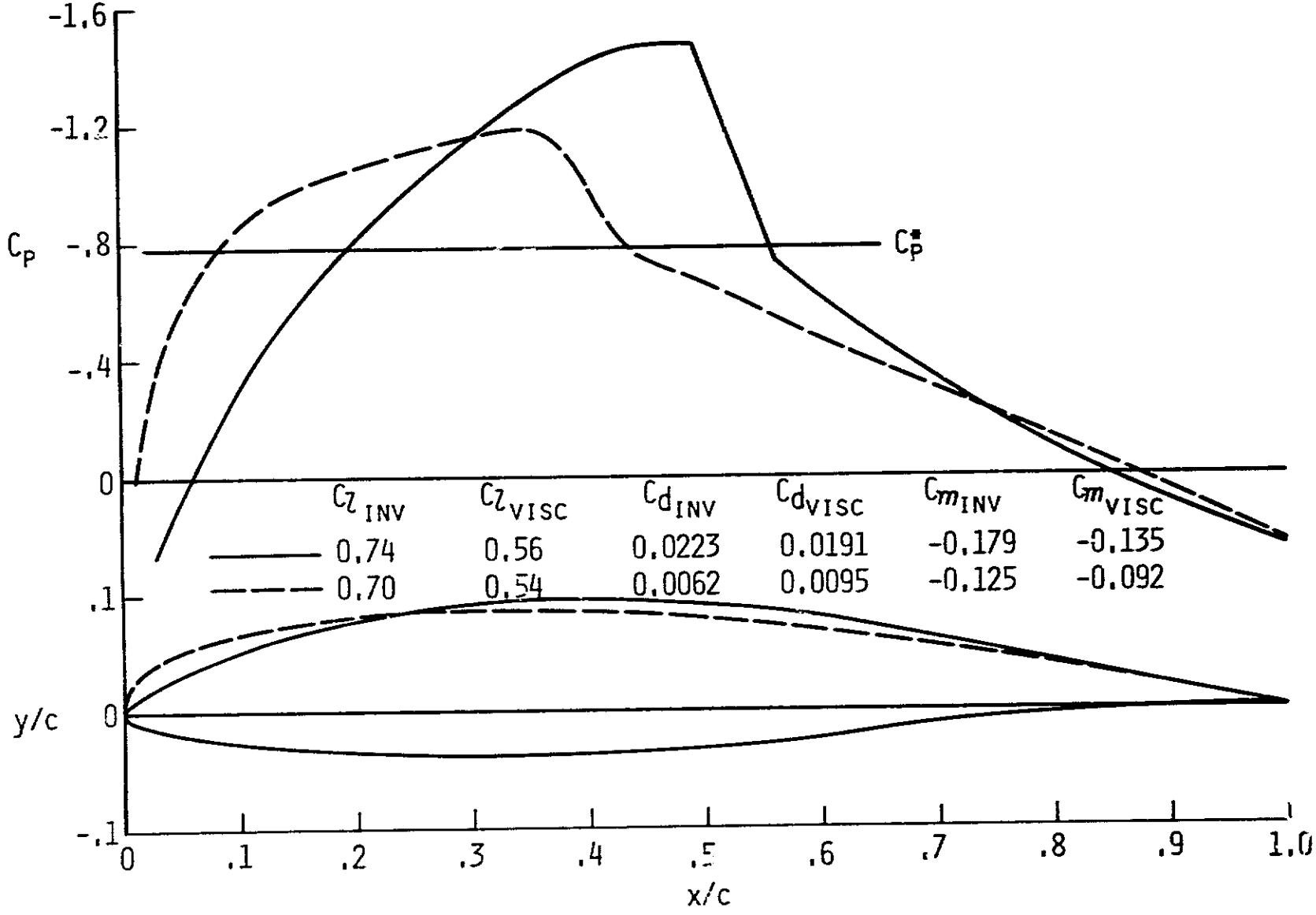

(b) Re = 20×10^6

Fig. 4 - Concluded

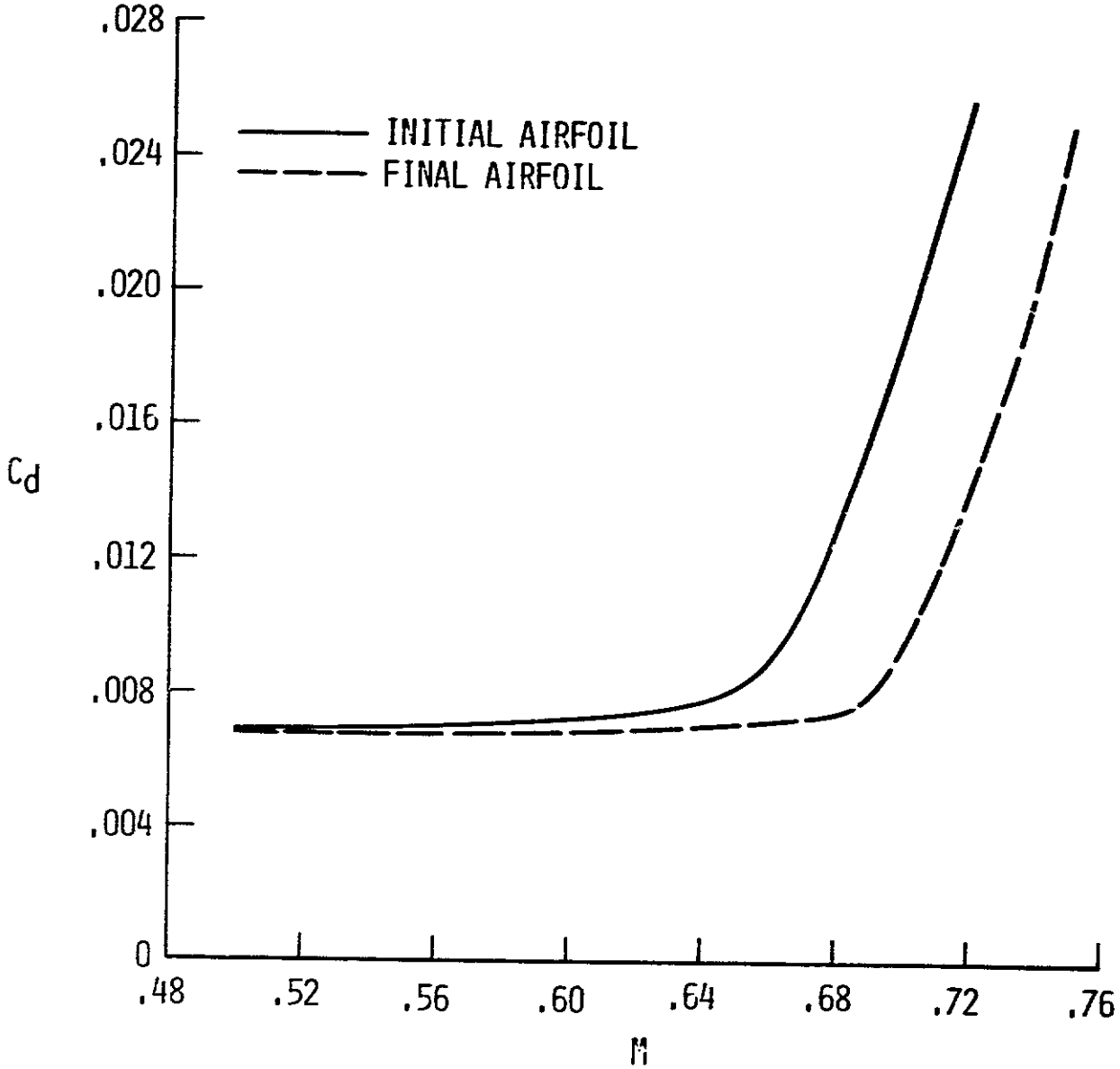

Fig. 5 - Mach number effect on the drag characteristics of the airfoils shown in figure 3; Re = 20×10^6, $\alpha = 0°$

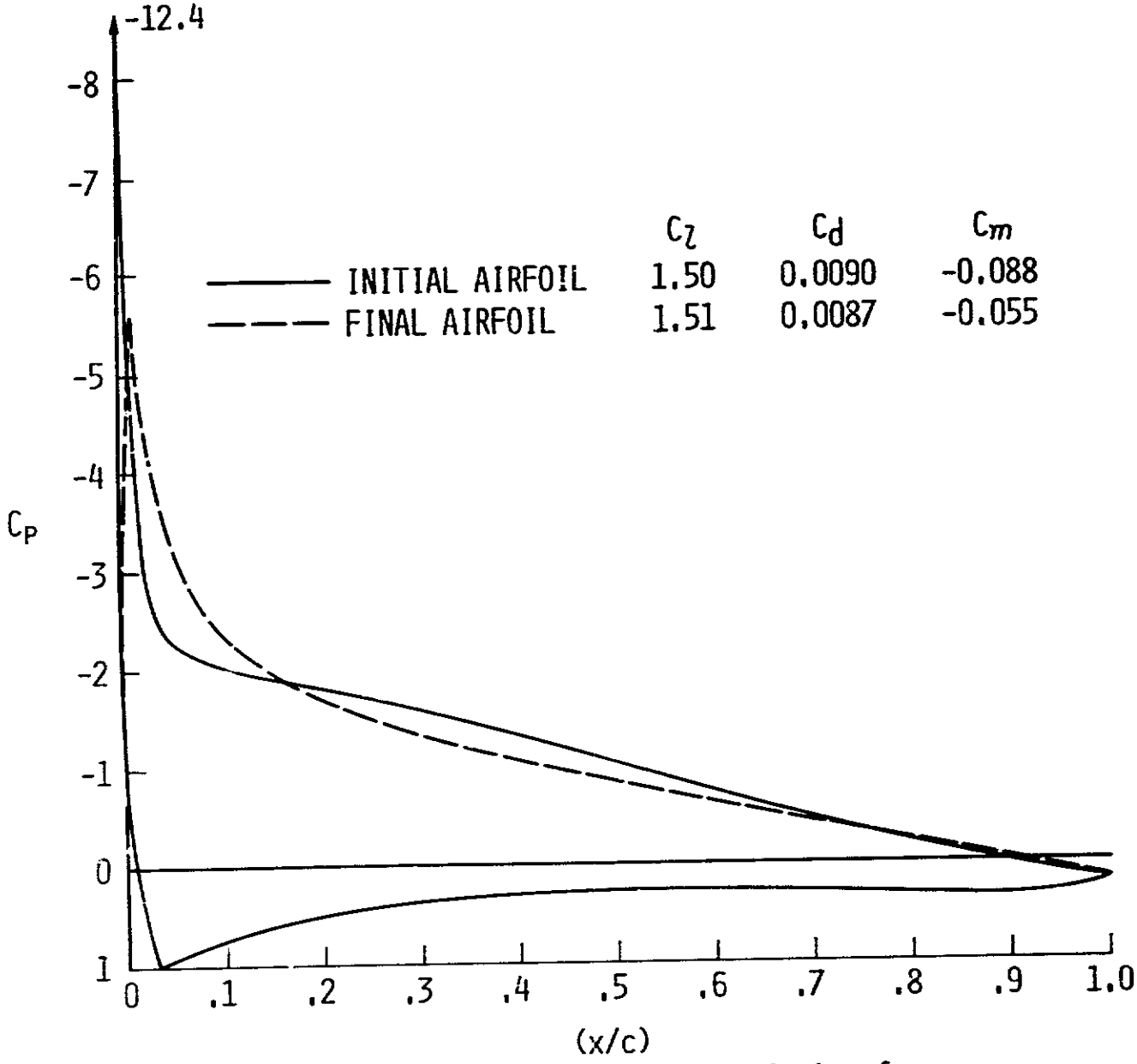

Fig. 6 - Low speed pressure distributions for the airfoils shown in figure 3; M = 0.1, Re = 10×10^6, $\alpha = 0°$

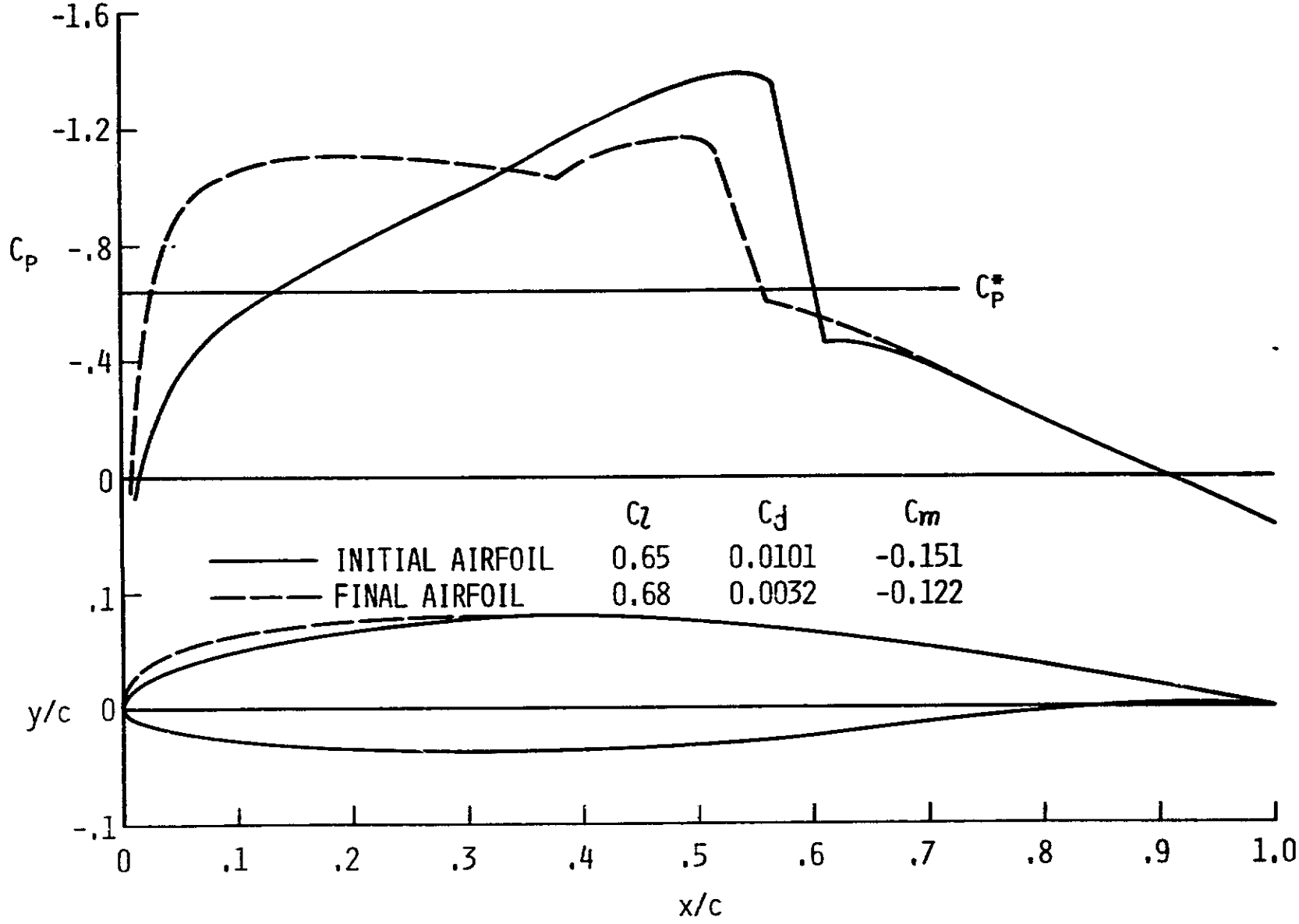

Fig. 7 - Inviscid drag minimization; M = 0.72, $\alpha = 0°$

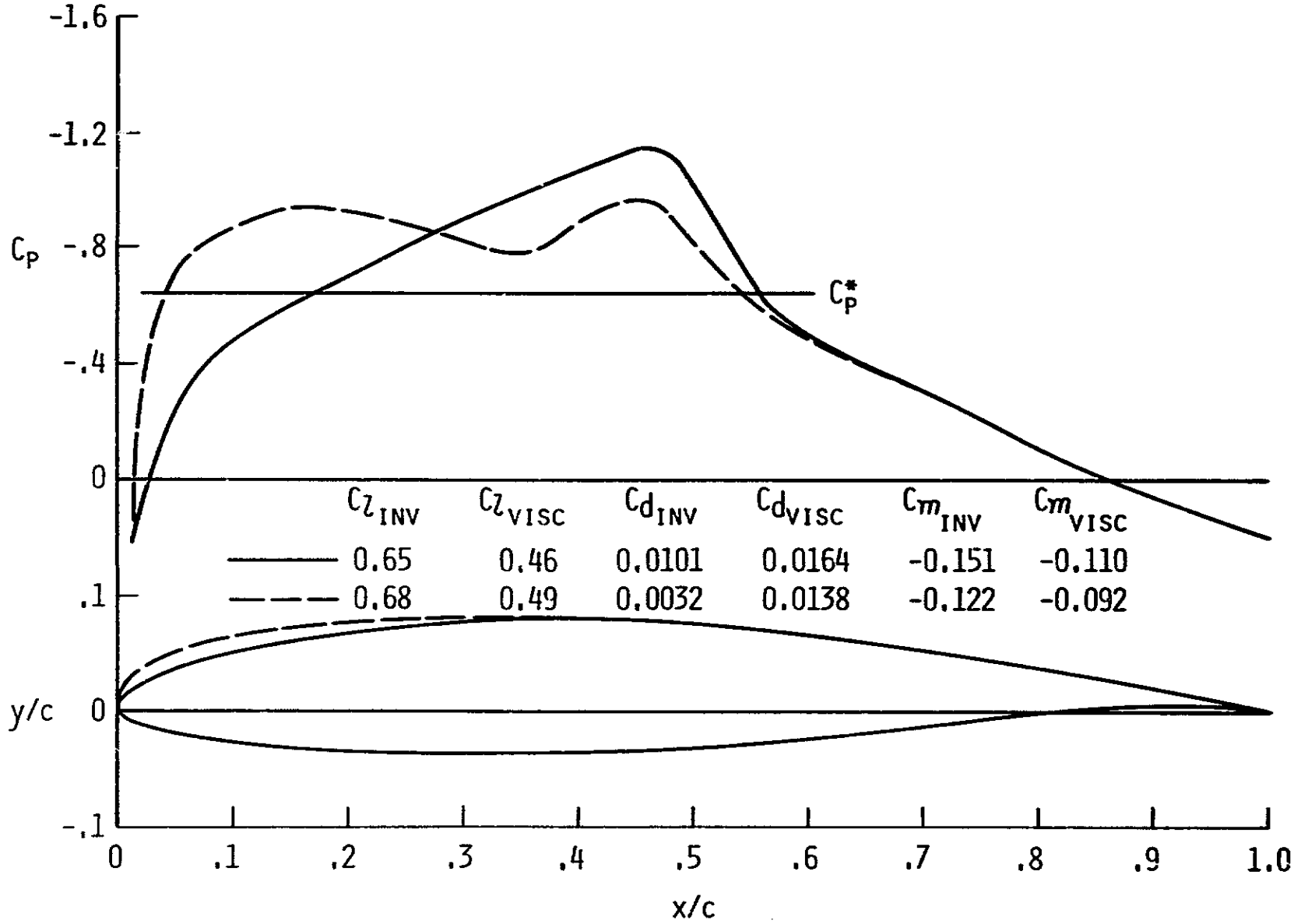

(a) Re = 1.3×10^6

Fig. 8 - Aerodynamic characteristics of the airfoils shown in figure 7 with boundary-layer correction; M = 0.72, $\alpha = 0°$

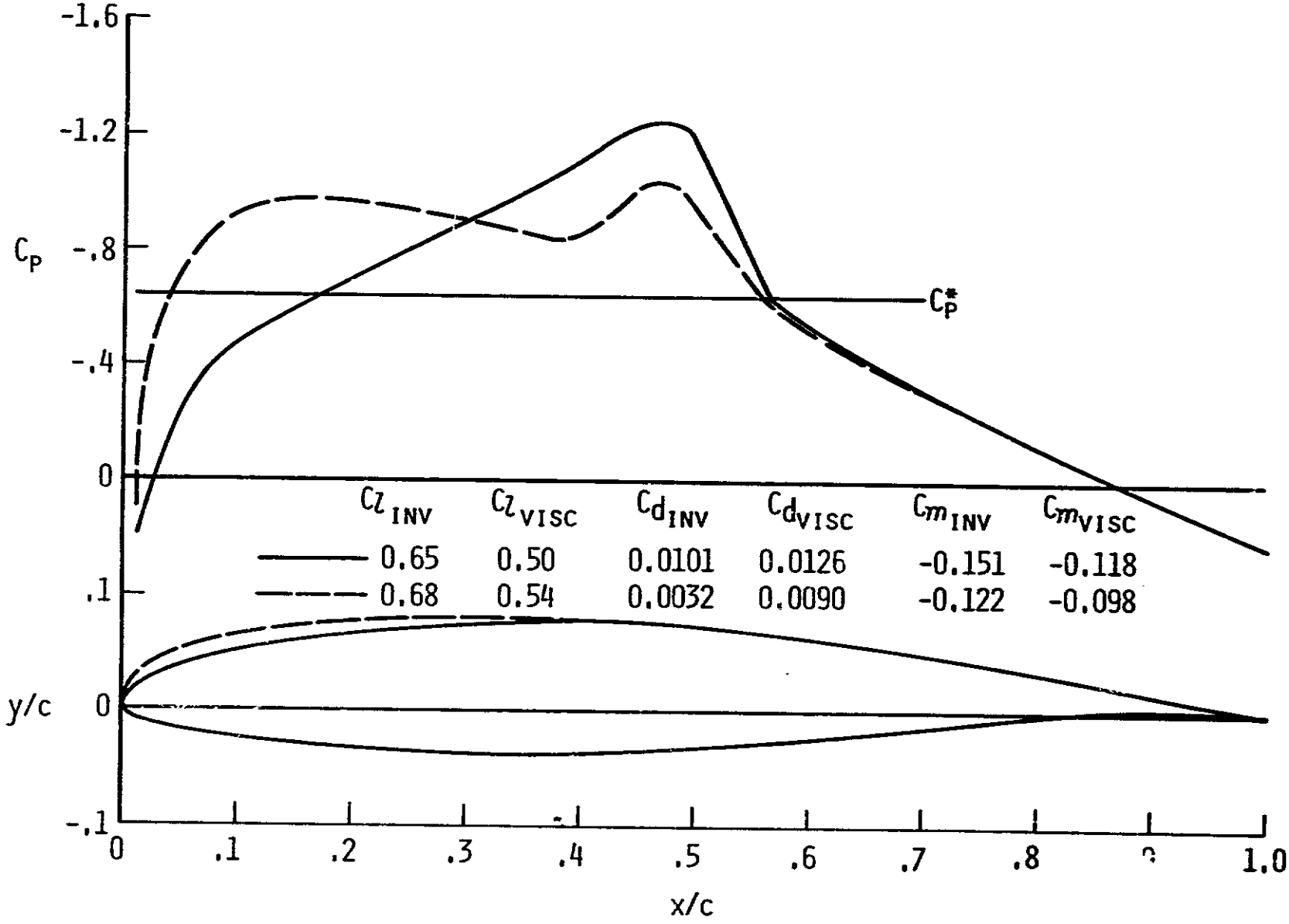

(b) Re = 20×10^6

Fig. 8 - Concluded

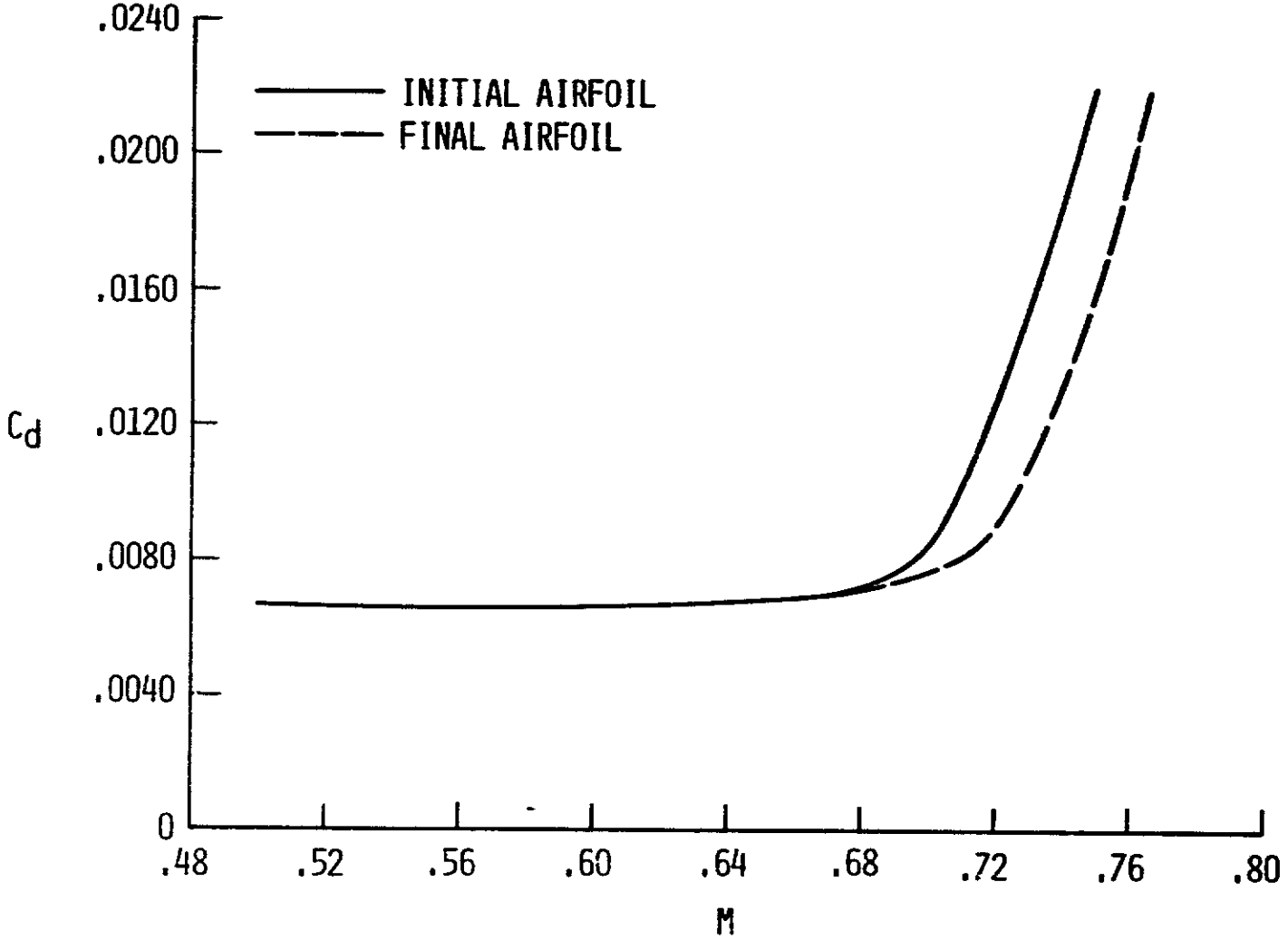

Fig. 9 - Mach number effect on the drag characteristics of the airfoils shown in figure 7; Re = 20×10^6, $\alpha = 0^\circ$

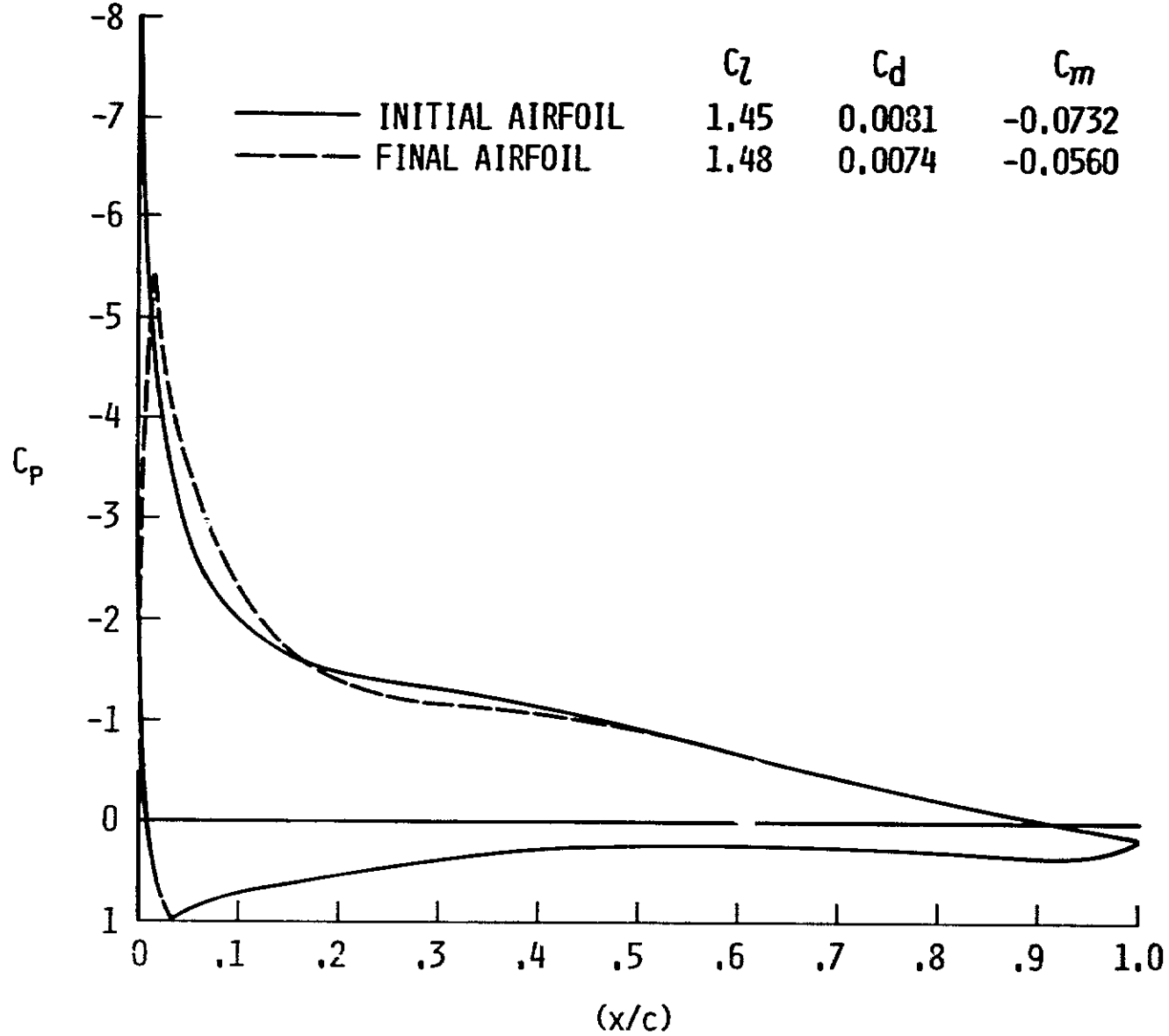

Fig. 10 - Low speed pressure distributions for the airfoils shown in figure 7; M = 0.1, Re = 10×10^6, $\alpha = 10^\circ$

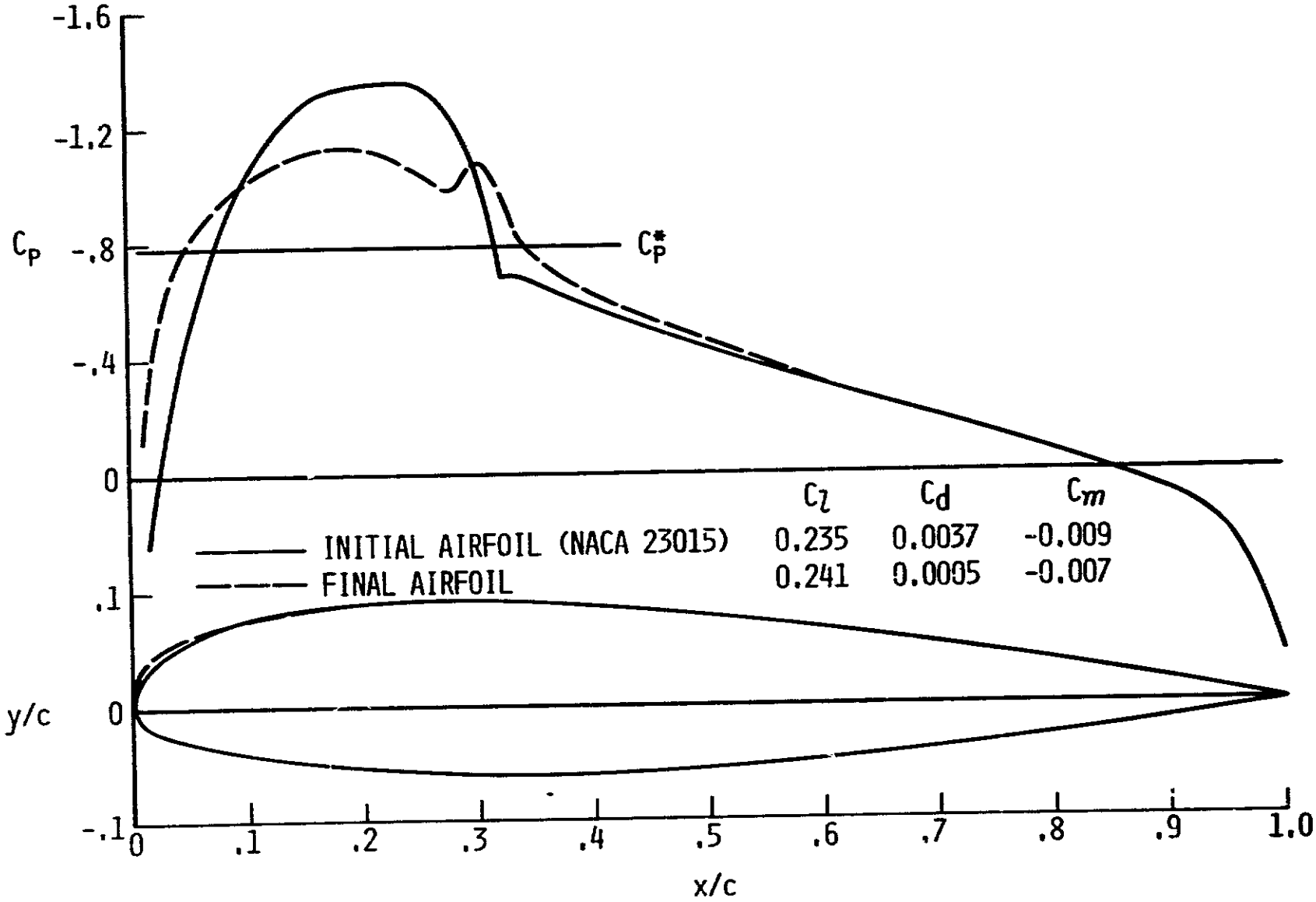

Fig. 11 - Inviscid drag minimization; M = 0.7, $\alpha = 0°$

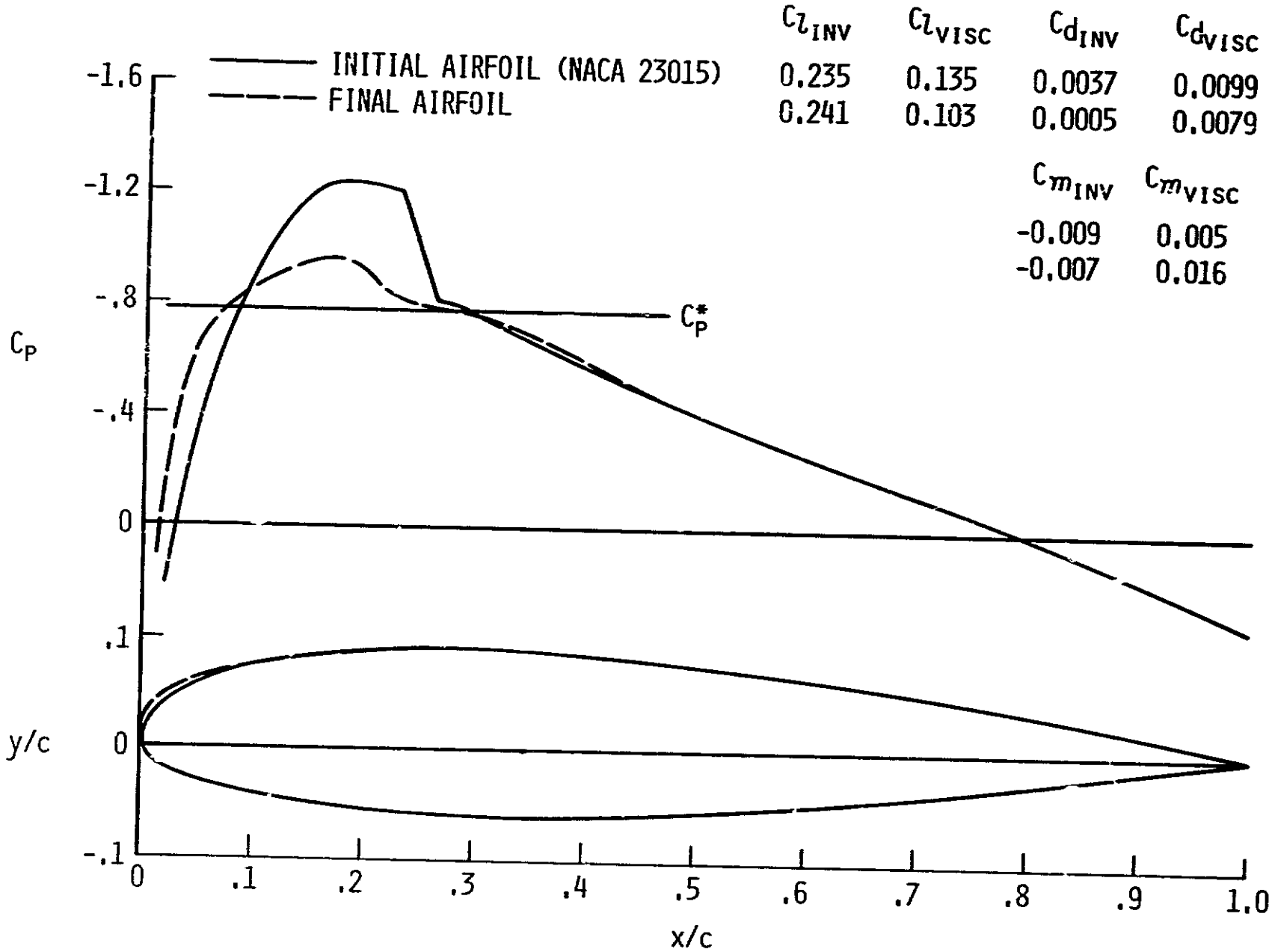

Fig. 12 - Aerodynamic characteristics of the airfoils shown in figure 11 with boundary-layer correction; M = 0.7, Re = 10×10^6, $\alpha = 0°$

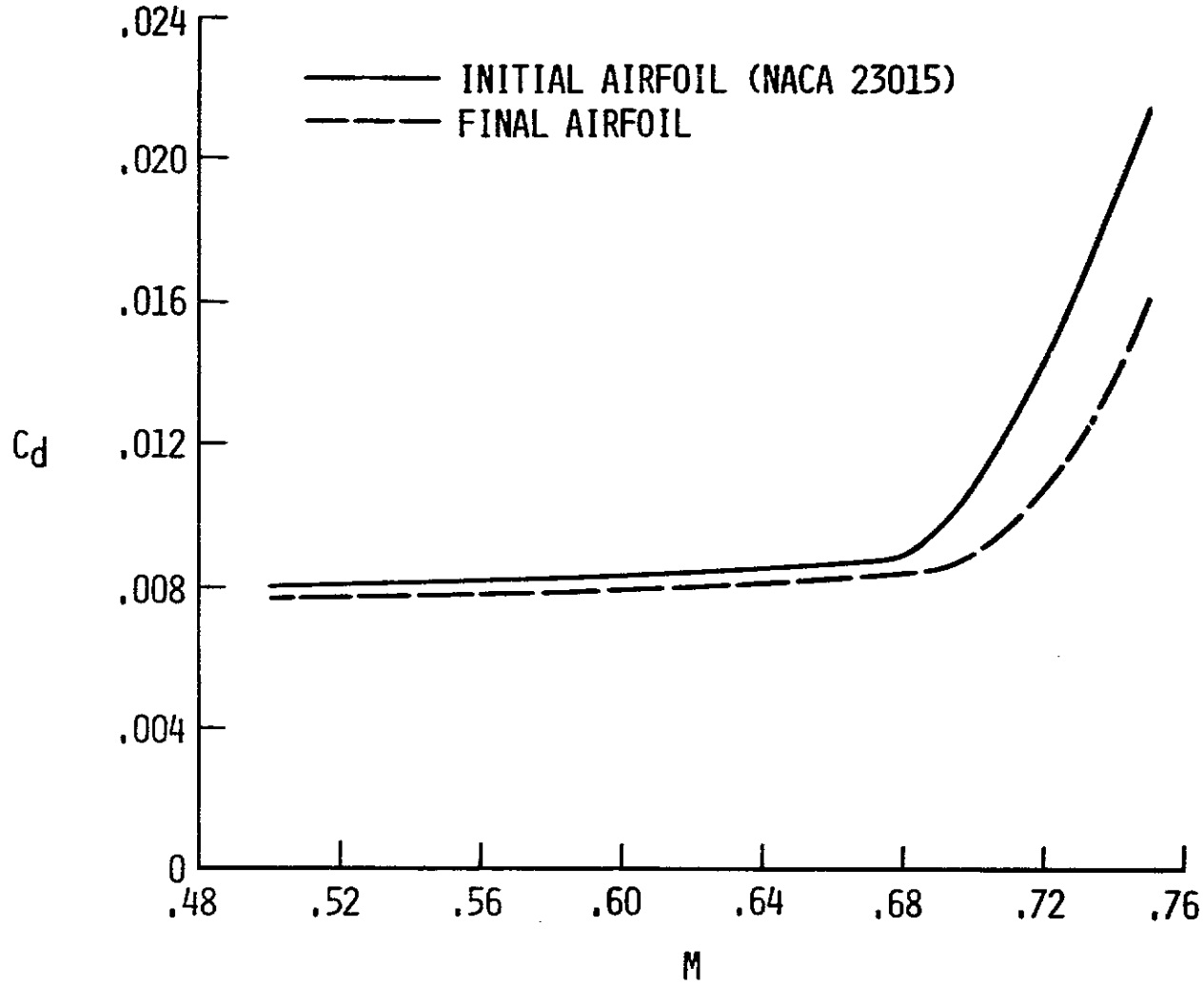

Fig. 13 - Mach number effect on the drag characteristics of the airfoils shown in figure 11; Re = 20×10^6, $\alpha = 0°$

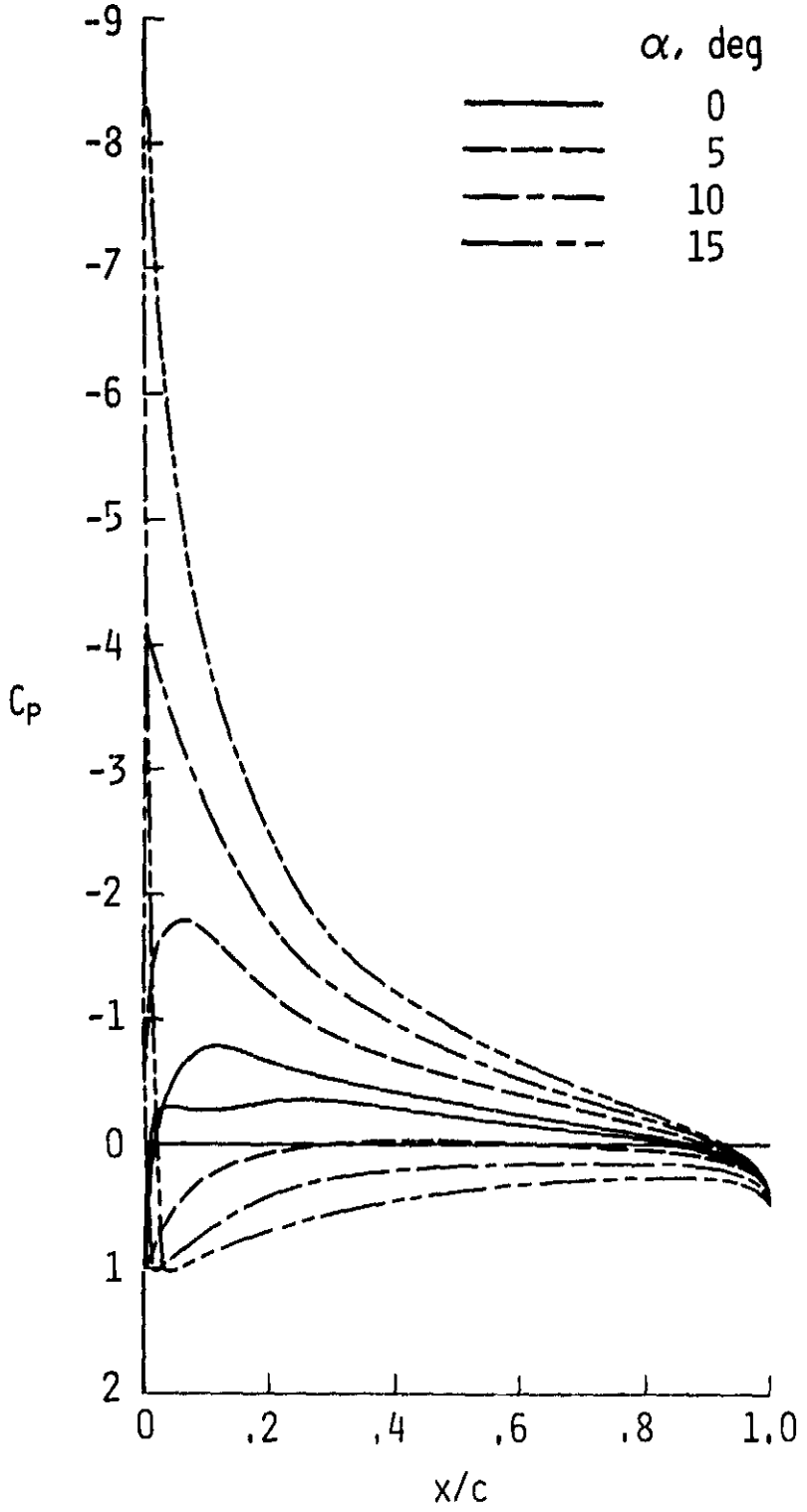

Fig. 14 - Inviscid low speed pressure distributions for NACA 23015 airfoil; M = 0.1

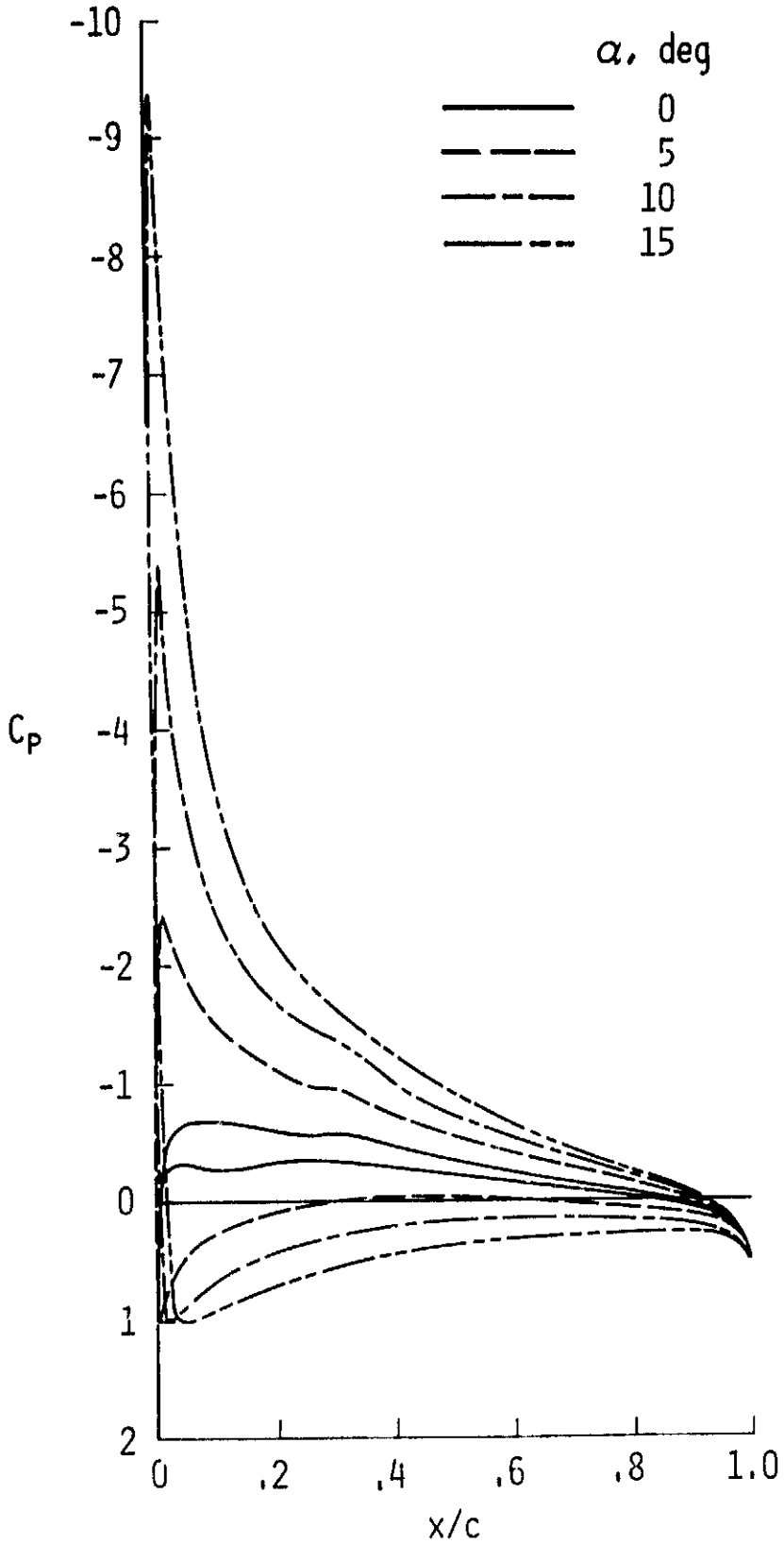

Fig. 15 - Inviscid low speed pressure distributions for the modified NACA 23015 airfoil; M = 0.1

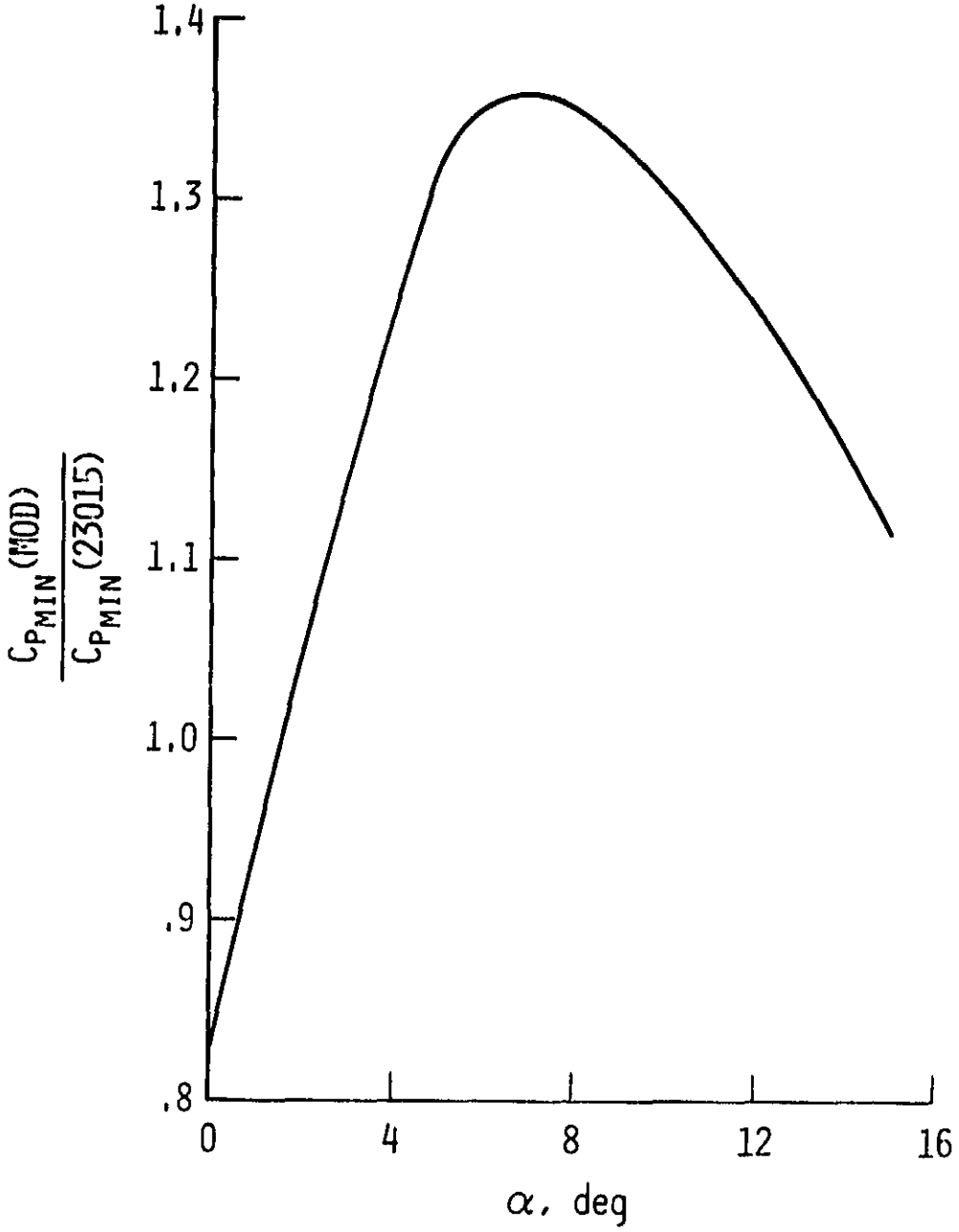

Fig. 16 - Ratio of $C_{p_{min}}$ for the NACA 23015 airfoil to $C_{p_{min}}$ for the modified 23015 airfoil; M = 0.1

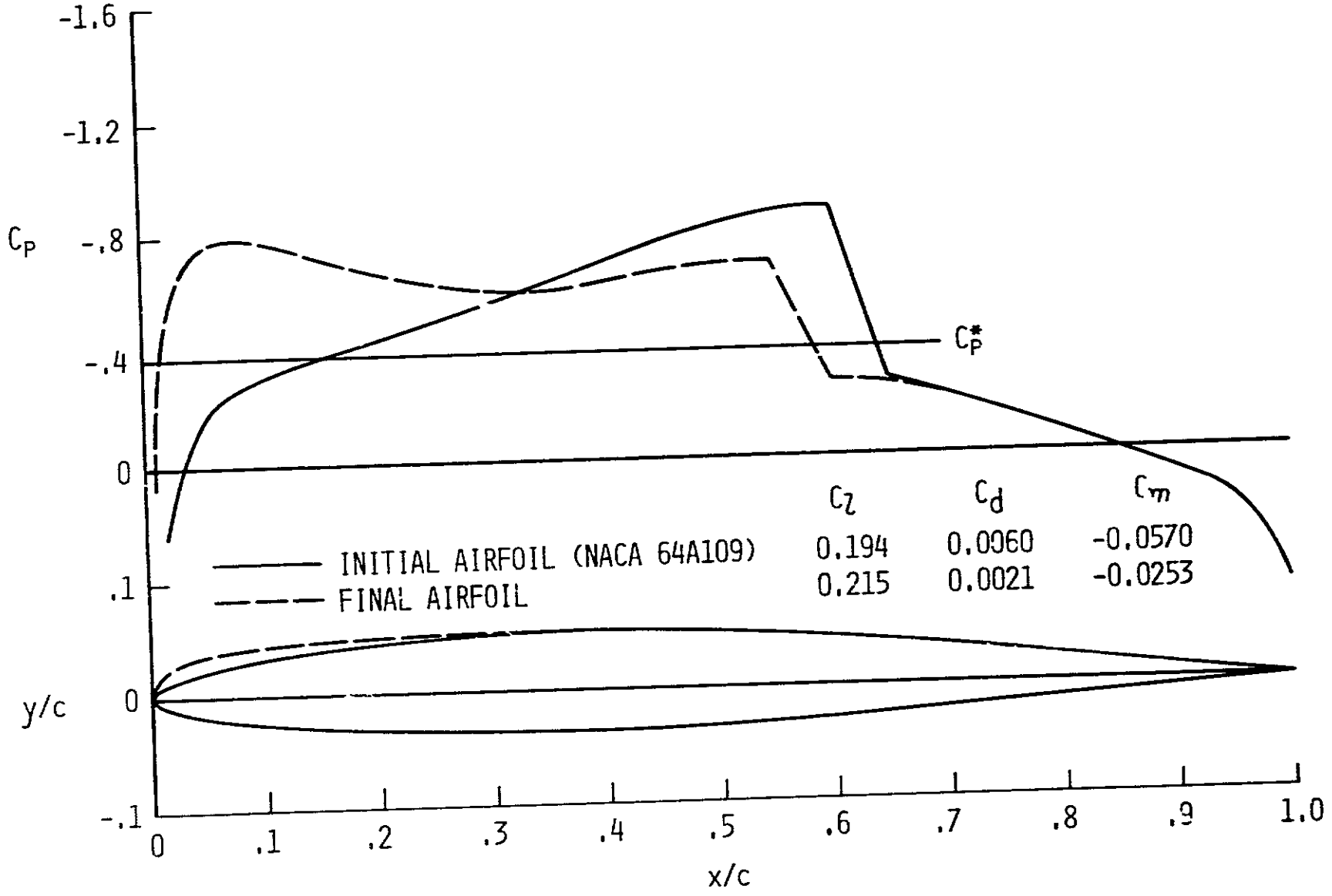

Fig. 17 - Inviscid drag minimization; M = 0.82, $\alpha = 0°$